IEEE Access
Multidisciplinary | Rapid Review | Open Access Journal

Received October 18, 2018, accepted November 3, 2018, date of publication November 12, 2018,
date of current version December 18, 2018.

Digital Object Identifier 10.1109/ACCESS.2018.2880447

Design and Performance Analysis of Power Line Communication Networks Under Impulsive Noise in Smart Home

YUWEN QIAN[1], XIANGWEI ZHOU[2], JUN LI[1], FEIXIANG ZHANG[2], LONG SHI[3], (Member, IEEE), AND FENG SHU[1]

[1]School of Electronic and Optical Engineering, Nanjing University of Science and Technology, Nanjing 210094, China
[2]Division of Electrical and Computer Engineering, Louisiana State University, Baton Rouge, LA 70803, USA
[3]Science and Math Cluster, Singapore University of Technology and Design, Singapore 487372

Corresponding author: Yuwen Qian (admon@njust.edu.cn)

ABSTRACT Power line communication (PLC) is an attractive approach to provide information transfer services for the smart home. The PLC network inherently suffers from the severe channel fading and impulsive noise. According to the mode of impulsive and the impulsive occurrence, the PLC channel can be modeled as the channel with memory. We compute the achievable rate by employing the Markov process with a finite number of states based on the dependence among the impulsive occurrence numbers in different time slots. Furthermore, the cumulative distribution function (CDF) for the received signal-to-noise ratio is derived with the statistical characteristics of the PLC channel. This helps in obtaining the ergodic capacity and outage probability for the PLC channels. We finally present the simulation results to verify the analytical results.

INDEX TERMS Achievable rate, impulsive noise, outage probability, power line communications, smart home.

I. INTRODUCTION

Power line communication (PLC) can provide Internet access for various types of electrical devices, which has attracted great attention recently and enabled wide applications in the smart grids. In the past few years, the dramatic development of the access network in electrical medium-voltage has led to the broadband PLC. Nowadays, the data rate in the broadband PLC can be up to around two Gbps [1]. At the same time, the narrow-band PLC is considered as a promising communication technology for smart home applications, such as power meter reading, electrical equipment auto-controlling, and networking of consumer appliances [2].

However, PLC encounters a more hostile environment when compared with the conventional wired and wireless communications due to severe signal fading and impulsive noises [3]. In general, the impulsive noise in PLC channel occurs randomly with a short duration and a high power spectral density [4]. Therefore, the signal-to-noise ratio (SNR) of the PLC channel falls dramatically in the presence of impulsive noises. In addition, the multi-path effect is the serious problem, which causes the frequency selective fading [5], [6]. Furthermore, the PLC networks are branch-based topology. As a result, transmitted signals are reflected at connected pointed, capacitor banks, and transformers, which results in fast fading [7]. In this case, performance evaluation, especially the capacity analysis, for the PLC channel becomes a crucial topic.

Initially, the performance analysis for PLC channels mainly focus on the measurements of the coherence bandwidth [8]. The basic idea of this approach is that the bandwidth of the coherence bandwidth is broader than the transmitted signal. According to the transmission line theory [9], a distance-based signal attenuation channel model has been developed and the capacity of the PLC channel has been further estimated in [10]. Although this specific data-based performance analysis is accurate in particular cases, it cannot be generalized. In this case, the distance-based statistical channel model has been introduced in [11] to generalize the performance analysis. Similarly, a statistical PLC channel model has been proposed in [12], where the PLC channel is considered as the combination of several PLC sub-channels with log-normal fading.

Recently, the performance analysis of the PLC channel with impulsive noises has drawn tremendous

interests [13]–[15]. Reference [14] is one of the representative studies that tackle this fundamental issue with Gaussian signaling to approximate the impulsive noise. Nonetheless, the method cannot be applied in the low-power region. In this case, the impulsive noise in the PLC channel is modeled as the Bernoulli-Gaussian noise [16], [17], in which channel noise is considered as the combination of the impulsive and Gaussian noises. As a result, PLC systems run in either of the two noise states, which are the Gaussian noise and impulsive noise states. With the computation of the differential entropy of the system for these two states, the capacity can be derived [16]. In addition, the performance analysis for the PLC channel under Bernoulli-Gaussian noise has been discussed in [17], where the performance analysis is conducted by approximating the impulsive noise as the sum of several Gaussian noises with zero mean and constant variances [1]. However, the number of the Gaussian noises is assumed to be constant, which unfortunately is not practical, since the impulsive noise in a PLC system depends on the number of turning on/off of electrical equipment that vary dynamically, which leads to the variation of the number of the Gaussian noises used to approximate the impulsive noise.

An effective approach to solving the problem is to adopt the Middleton class-A noise model, in which the impulsive noise is described with several states. To distinguish different impulsive noise states, the impulsive occurrence number (ION) in a time slot is used as the index. Similarly, the impulsive noise modeled as the Middleton class-A noise can also be approximated as the sum of the Gaussian noises. However, in different states, there are different numbers of Gaussian noises used to approximate the impulsive noise, corresponding to the various numbers of turning on/off of electrical equipment. For this reason, the Middleton class-A modeled noise is a more accurate estimate of the impulsive noise than the Bernoulli-Gaussian model according to the comparison in [18]. With the Middleton class-A model, the closed-form expressions of the bit error rate (BER) and capacity for the PLC channel have been derived in [19] by computing the average mutual information for each noise state. Moreover, the point-to-point PLC has been studied in [1], where the signal model with OFDM has been formulated and the upper and lower capacity bounds for the PLC channel under impulsive noise have been further derived. However, the ION is considered to follow Poisson distribution and thus different noise states are independent. Nonetheless, different noise states are generally not independent in PLC systems since they correspond to the turning on/off of related electrical equipment.

To establish a practical model for the impulsive noise channel, where noise states are non-independent, a Markov process is adopted to describe the Middleton class-A modeled impulsive noise [5], [19], [20]. Generally, the current state can be estimated by the previous states in a Markov process [5]. Inspired by this idea, the ergodic capacity for the impulsive noise modeled as the Middleton class-A noise has been derived in [19]. Similarly, the performance of a multiple input multiple output (MIMO) PLC system has been analyzed in [20], where the impulsive noise is modeled as a two-state Markov process. However, the Markov states in these studies are assumed independent to avoid complex computation. Therefore, performance analysis for the impulsive noise with non-independent states in the PLC channel is still a challenge.

In this paper, we model the impulsive noise with the Middleton class-A model and the PLC channel is modeled as a memory channel. We use Markov processes to describe the PLC channel with memory, and then derive the achievable rate, ergodic capacity, and outage probability. In particular, we list our five-fold contributions below.

- We model the PLC channel with memory as a Markov process, where the Markov states are mutually dependent. By using the finite state memory channel FSMC) theory [21], we derive the closed-form expression of the achievable rate for the PLC channel with memory.
- With the combination of PLC sub-channels, we formulate the fading of the PLC channel as a log-normal sum function, which is approximated by a specific exponential function to derive the cumulative distribution function (CDF) of the received SNR.
- Based on the derived CDF of the received SNR for the PLC channel, we derive the ergodic capacity and outage probability for the PLC channels with the Taylor's extension and Hermite polynomial.

The remainder of this paper is organized as follows. In Section II, the PLC system and channel models are described. In Sections III, we derive the closed-form expressions of the achievable rate for the PLC channel with memory. Then we use the results of Sections III to evaluate the ergodic capacity and outage probability for the PLC channel with memory in Sections IV. In Section V, we present the numerical results. Finally, we summarize the main findings in Section VI.

II. PLC CHANNEL AND SYSTEM MODEL

A. PLC CHANNEL MODEL

As shown in Fig. 1, we design a smart home PLC infrastructure that composes of several sub-circuits. In addition, the single-phase transformer is adopted to isolate the sub-circuits, which is suitable for the smart home users due to its low cost and small size. Such a structure can bring safe power utility and convenient maintenance for smart home users. In the system, there are several parallel power lines used for different sub-circuits. Hence, we use these power lines to transmit signals simultaneously to improve data rate. Furthermore, due to the isolation with the transformer, the transmitting signals over power lines in different sub-circuits do not interfere with each other. Therefore, signals can be transmitted from the transmitter to the receiver via multiple sub-circuits independently. In this case, we model the PLC channel with diversity PLC sub-channels, as shown in Fig. 2.

As shown in Fig. 2, there is a buffer used by the transmitter and receiver respectively to collect the transmitting data.

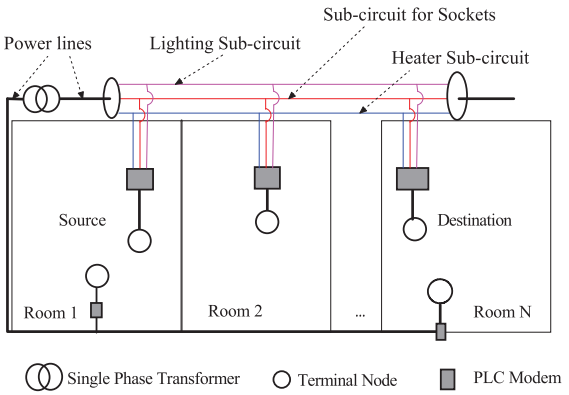

FIGURE 1. A typical PLC network of smart home connected with several power lines, where a single-phase transformer is used to isolated different sub-circuits.

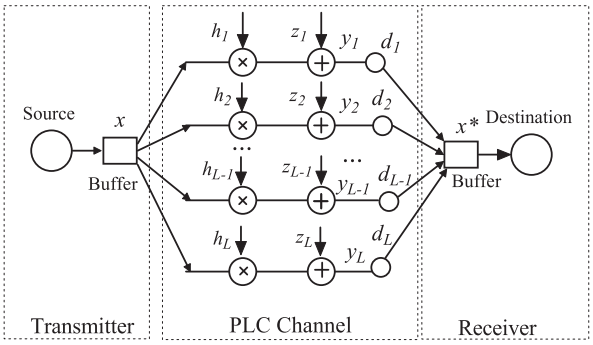

FIGURE 2. The PLC channel model with L diversity sub-channels, where x is the input symbol, x^* is the output signal, h_l, z_l, d_l, and y_l ($1 \le l \le L$) are the channel gain, received noise, signal detector, and received signal of the lth PLC sub-channel.

In addition, we adopt the binary phase shift keying (BPSK) to modulate symbols transmitting via the L PLC sub-channels. The receiver can receive the symbols from these sub-channels by combining them from frequency, time, and space. Hence, the L sub-channels can be treated as one PLC channel.

In the PLC system, the input signal is transmitted via the L sub-channels from the transmitter to the receiver. The received signal y_l of the lth ($1 \le l \le L$) sub-channel is

$$y_l = h_l x_l + z_l, \tag{1}$$

where x_l is the signal transmitted via the lth sub-channel, z_l is the received noise of the sub-channel, and h_l is the channel gain of the sub-channel.

We use the maximal-ratio combining (MRC) [22] to combine the L sub-channels as one PLC channel. Then we can obtain the optimal received SNR of the PLC channel as

$$\gamma = \frac{P_s}{\sigma^2} \frac{\left(\sum_{l=1}^{L} w_l \cdot h_l\right)^2}{\sum_{l=1}^{L} w_l^2}, \tag{2}$$

where γ is the received SNR, w_l is the weight for the lth sub-channel, P_s is the transmit power, and σ^2 is the channel noise variance.

Let w_l be proportional to the gain of the lth sub-channel. Specifically, we define $w_l = \mu \times h_l$, where μ ($\mu \le 0$) is a constant. We define $\gamma_p \triangleq \frac{P_s}{\sigma^2}$ and the received SNR is given as

$$\gamma = \gamma_p \sum_{l=1}^{L} h_l^2. \tag{3}$$

The noise in the combined PLC channel, according to [4] and [13], is considered as a combination of the Gaussian and impulsive noises, i.e.,

$$z = z_g + z_w, \tag{4}$$

where z_g and z_w are the Gaussian and impulsive noises.

B. SYSTEM MODEL

PLC systems have recently been widely deployed in buildings, homes, and enterprises. In these places, electrical equipment is frequently turned on/off, which generates a lot of impulses. Moreover, frequency conversion equipment, such as air-conditioners, can also generate impulses when shifting working frequencies.

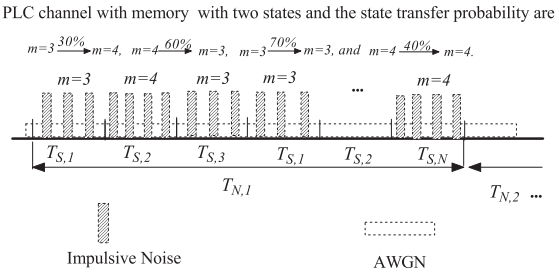

FIGURE 3. The occurrence modes of the impulsive noise, where m is the state index that equals the ION of the time slot, $T_{S,i}$ is time duration of the time slot for a system state, and $T_{N,i}$ is the time duration for transmitting N symbols.

In practical PLC systems, the IONs are non-independent with those of the previous time slots. Let us take a building with a constant number of switches as an example. When different numbers of these switches are dynamically turned on/off, different numbers of impulses are generated. The number of switches turned on/off in a time slot is predictable according to the numbers of switchers turned on/off in the previous time slots. As a result, the ION of the current time slot is relevant to the IONs of the previous time slots. Therefore, we use two noise states in Fig. 3 as an example, where the ION is three and four impulsive occurrences. In this system, the PLC channel under impulsive noise with non-independent IONs can be considered as a channel with memory and has a finite number of states.

According to [23], since the PLC channel can be considered to be quasi-stationary (or quasi cyclostationary), the channel state information (CSI) can be obtained by the terminal nodes by using a feedback channel. If the ION in one time slot is m ($0 \le m \le M-1$), we use m different Gaussian noises to approximate the impulsive noise. In this scenario,

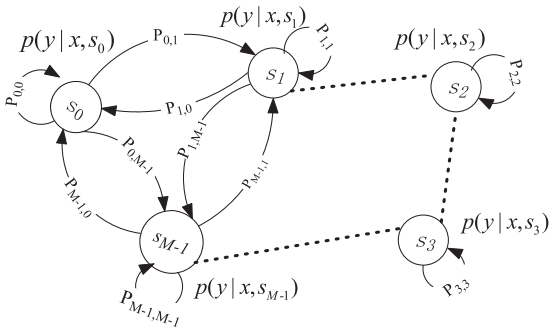

FIGURE 4. The application of the Markov chain with a finite number of states to the PLC system with impulsive noise. $P_{i,j}$, $0 \le i, j \le M-1$, denotes the transition probability from the ith state to the jth state, s_i represents the ith state, and $P_i(y|x, s_i)$ denotes the conditional probability of the ith state of the output y conditioned on x.

we model the PLC channel with memory as a non-redundant and periodic stable Markov process with a finite number of states as shown in Fig. 4. Here, we use system state m to represent ION m in the time slot.

In the Markov process, the state set is defined as

$$U = [s_0, \cdots, s_m, \cdots, s_{M-1}]^{\mathcal{T}}, \tag{5}$$

where s_m represents the system in the mth state and $\mathcal{T}$ is the transposition operator.

In the system, the Markov chain is positive recurrent and ergodic. Let U_n be the system state at time slot n and P be the transition probability matrix. Then we have

$$P_{i,j} = \Pr\left(U_{n+1} = s_j | U_n = s_i\right), \tag{6}$$

where s_i and s_j are the states in U and $P_{i,j}$, $0 \le i, j \le M-1$, represents the state transition probability that the system shifts from the ith state at time slot n to the jth state at time slot $n+1$.

We define β_m as the occurrence probability of the mth state. According to [19], the PDF of the impulsive noise in the PLC channel with memory modeled with a M-state Markov process can be given as

$$f_z(z) = \sum_{m=0}^{M-1} \frac{\beta_m}{\sqrt{2\pi\sigma_m^2}} e^{-\frac{x^2}{2\sigma_m^2}}, \tag{7}$$

where σ_m^2 is the variance of the noise in the mth state.

III. ACHIEVABLE RATE ANALYSIS

In the PLC channel with memory shown in Fig. 4, the probability of the current state can be predicted by the past inputs and outputs. Therefore, we can calculate the achievable rate for the PLC system according to its past inputs and outputs. Since the transmitting and receiving buffers are equipped for the transmitter and receiver of PLC channels as in Fig. 2, the past inputs and outputs can be obtained in the buffers.

Let x_n and y_n be the input and output of the PLC channel with memory at time n, respectively. According to (6) and Fig. 4, the output probability conditioned on the input and system state at time n is

$$\Pr(y_n|x_n, U_n) = \sum_{m \in U} p_m(y_n|x_n)\, I(U_n, s_m), \tag{8}$$

where U_n is the current state of the system at time n, $p_m(y|x) = \Pr(y|x, U = s_m)$, and $I(U_n, s_m)$ is

$$I(U_n, s_m) = \begin{cases} 1, & U_n = s_m, \\ 0, & U_n \ne s_m. \end{cases} \tag{9}$$

We use the form $b^n \triangleq (b_1, ..., b_n)$ for $b_i = x, y$, or U for $i = 1, ..., n$. Since the current state is independent with the previous inputs and outputs, we have

$$p\left(U_{n+1}|U_n, x^n, y^n\right) = p\left(U_{n+1}|U_n\right). \tag{10}$$

Since the PLC channel is considered to be memoryless for each state, we have

$$p\left(y_{n+1}|U_{n+1}, x_{n+1}, U^n, x^n, y^n\right) = p\left(y_{n+1}|U_{n+1}, x_{n+1}\right). \tag{11}$$

With the assumption that x_n is independent of the previous inputs and outputs, we have

$$p\left(y_{n+1}, x_{n+1}|U_{n+1}, U^n, x^n, y^n\right) = p\left(y_{n+1}, x_{n+1}|U_{n+1}\right). \tag{12}$$

Combining (10) and (12), we obtain

$$p\left(y^N, x^N|U^N\right) = \prod_{n=1}^{N} p\left(y_n, x_n|U_n\right). \tag{13}$$

Similarly, from (11) and (13) we have

$$p\left(y_{n+1}|U_{n+1}, U^n, y^n\right) = p\left(y_{n+1}|U_{n+1}\right). \tag{14}$$

Here we define $\boldsymbol{\rho}_n = (\rho_n(1), ..., \rho_n(M))$ as an M-dimensional conditional state distribution vector conditioned on the outputs and $\boldsymbol{\varsigma}_n = (\varsigma_n(1), ..., \varsigma_n(M))$ as the M-dimensional conditional state distribution vectors condition on the outputs and inputs, where

$$\rho_n(m) = p\left(U_n = s_m|y^{n-1}\right) \tag{15}$$

and

$$\varsigma_n(m) = p\left(U_n = s_m|x^{n-1}, y^{n-1}\right). \tag{16}$$

With $\boldsymbol{\rho}$ and $\boldsymbol{\varsigma}$, the achievable rate of the PLC channel with memory can be obtained by Theorem 3.

Theorem 1 Given N ($N \to \infty$) inputs and outputs, the achievable rate of the PLC channel with memory R_{mry} is

$$R_{mry} = \frac{1}{N} \sum_{n=1}^{N} \left(\log \sum_{m=0}^{M-1} \left(\frac{(1+\gamma_m)\rho_n^2(m)}{\varsigma_n^2(m)} \right) \right), \tag{17}$$

where γ_m is the received SNR for the channel in the mth state.

Proof: See Appendix A. ■

Theorem 1 provides a method to estimate the achievable rate of a PLC channel with memory. According to (17),

we notice that the achievable rate depends on ς_n and ρ_n. In the following, a recursive method is employed to calculate these two conditional probabilities.

First, we set the initial values of $\boldsymbol{\varsigma}$ and $\boldsymbol{\rho}$ as

$$\boldsymbol{\rho}_0 = \boldsymbol{\varsigma}_0 = \left(p\left(U_0 = s_1\right), p\left(U_0 = s_2\right), ..., p\left(U_0 = s_N\right)\right), \tag{18}$$

where $p(U_0 = s_i)$ represents the probability that the system is at the ith state initially. $p(U_0)$ equals the occurrence frequency of state s_i.

Second, by using Bayes' rule, we have

$$p\left(U_n|x^n, y^n\right) = \frac{p\left(y_n|U_n, x_n\right) p(x_n|x^{n-1})}{p\left(x^n, y^n\right)} \times p\left(U_n|x^{n-1}, y^{n-1}\right) p\left(x^{n-1}, y^{n-1}\right), \tag{19}$$

where $p\left(x^n, y^n\right)$ is

$$p\left(x^n, y^n\right) = \sum_{m=0}^{M-1} p\left(x^n, y^n, U_n = s_m\right). \tag{20}$$

With (8) and (20), we have

$$p\left(x^n, y^n\right) = \sum_{m=0}^{M-1} p\left(y_n|x_n\right) p\left(x_n|x^{n-1}\right) p\left(U_n = s_m|x^{n-1}, y^{n-1}\right) p\left(x^{n-1}, y^{n-1}\right). \tag{21}$$

Substituting (21) into (19), we have

$$p\left(U_n|x^n, y^n\right) = \frac{p\left(y_n|U_m, x_n\right) p\left(U_n = s_m|x^{n-1}, y^{n-1}\right)}{\sum_{j=0}^{M-1} p\left(y_n|x_n, U_n = s_j\right) p\left(U_n = s_j|x^{n-1}, y^{n-1}\right)}. \tag{22}$$

Finally, the conditional probability for the mth state can be calculated with

$$\varsigma_{n+1}(m) = \frac{\sum_{j=0}^{M-1} p\left(y_n|x_n\right) \varsigma_n(j) P_{j,m}}{\sum_{l=0}^{M-1} p_l\left(y_n|x_n\right) \varsigma_n(l)}. \tag{23}$$

Similarly, we can utilize the following recursive formula to compute ρ_{n+1} as

$$\rho_{n+1}(m) = \frac{\sum_{j=0}^{M-1} p_j\left(y_i|U_i = s_j\right) \rho_n(j) P_{j,m}}{\sum_{l=0}^{M-1} p_l\left(y|U_n = s_j\right) \rho_n(l)}. \tag{24}$$

According to [21], the sequences $\boldsymbol{\varsigma}_n$ and $\boldsymbol{\rho}_n$ converge when the initial states are independent and the number of the initial states is finite. Due to the convergence of $\boldsymbol{\varsigma}_n$ and $\boldsymbol{\rho}_n$, the algorithm to calculate the achievable rate with (17) converges.

IV. ERGODIC CAPACITY AND OUTAGE PROBABILITY

In this section, we analyze the ergodic capacity of the PLC channel. For the analysis, the channel gain is assumed to vary across transmitted symbols and the duration of the communication time is assumed to be long enough for the channel to experience all states.

According to [12] and [24], the gain h_l of the PLC sub-channel in Fig. 2 follows a lognormal distribution with PDF $f_{h_l}(x)$ given as

$$f_{h_l}(x) = \frac{1}{\sqrt{2\pi\sigma^2}x} e^{-\frac{(\ln x - \mu)^2}{2\sigma^2}}, \tag{25}$$

where μ and σ^2 are the mean and variance of $\ln x$, which is a Gaussian random variable.

We define $\mu_\gamma = 2\mu$ and $\sigma_\gamma = 2\sigma$. Then the PDF of h_l^2 can be given as

$$f_{h_l^2}(x) = \frac{1}{\sqrt{2\pi{\sigma_\gamma}^2}x} e^{-\frac{\left(\ln x - \mu_\gamma\right)^2}{2{\sigma_\gamma}^2}}. \tag{26}$$

Define $t = \sum_{l=1}^{L} h_l^2$ and with [25] we can approximate the PDF of the received SNR as

$$f_t(x) \approx \frac{a_1 a_2 x^{-(a_2/\lambda+1)}}{\lambda\sqrt{2\pi}} \exp\left(-\frac{\left(a_0 - a_1 x^{-a_2/\lambda}\right)^2}{2}\right), \tag{27}$$

where $\lambda = \frac{\ln 10}{10}$ and a_0, a_1, and a_2 are constants.

With (27), we can obtain the CDF of the received SNR as

$$F_t(x) \approx \Phi\left(a_0 - a_1 x^{-a_2/\lambda}\right), \tag{28}$$

where $\Phi(x) = \int_0^x \frac{1}{\sqrt{2\pi}} e^{-\frac{t^2}{2}} dt$.

The closed-form expressions of ergodic capacity (in bits/s/Hz) for the PLC channel with memory are presented in Theorems 2. To derive the ergodic capacity for the PLC channel with memory, we assume that T_N, which is the time duration for the N inputs and outputs, is large enough to ensure that all the system states can be experienced.

Theorem 2 Given the PLC channel with memory under impulsive noise with a finite number of states, if the CSI and the noise states are open to the receiver, the ergodic capacity C_{mry} is

$$C_{mry} = \frac{1}{N}\sum_{n=1}^{N}\left(\log\left(\sum_{m=0}^{M-1}\frac{\rho_n^2(m)}{\sigma_m^2\varsigma_n^2(m)}\right) + \frac{1}{\sqrt{\pi}}\sum_{j=1}^{J} w_j \log\left(\frac{a_0 - \sqrt{2}q_j}{a_1}\right)^{-\lambda/a_2}\right). \tag{29}$$

Proof: See Appendix B. ■

The outage probability is defined as the probability that the data rate drops below an acceptable threshold T_R. The outage probability can be used as a crucial measure to the quality of service for PLC systems.

The outage probability of the PLC channel with memory P_{mry} is

$$\begin{aligned} P_{mry} &= P\left(R_{mry} < T_D\right) \\ &= P\left(\log\left(\sum_{m=0}^{M-1}\left(\frac{(1+\gamma_m)\,\rho_n^2(m)}{\varsigma_n^2(m)}\right)\right) < T_D\right) \\ &= P\left(\sum_{m=0}^{M-1}\left(\frac{(1+\gamma_m)\,\rho_n^2(m)}{\varsigma_n^2(m)}\right) < 2^{T_D}\right), \end{aligned} \tag{30}$$

where T_D is the threshold of the data rate for the PLC channel with memory. Then, (30) can be written as

$$\begin{aligned} P_{mry} &\approx P\left(t < 2^{T_D}/\sum_{m=0}^{M-1}\frac{\rho_n^2(m)}{\sigma_m^2\varsigma_n^2(m)}\right) \\ &= \Phi\left(a_0 - a_1\left(2^{T_D}/\sum_{m=0}^{M-1}\frac{\rho_n^2(m)}{\sigma_m^2\varsigma_n^2(m)}\right)^{-a_2/\lambda}\right). \end{aligned} \tag{31}$$

V. NUMERICAL RESULTS

In this section, we obtain numerical results with MATLAB and compare with the analytical results to verify our derivations. The parameters are chosen based on the HomePlug AV2 standard [26], tabulated in Table 1. Here the transmit SNR is defined as $P_s/\sigma^2(\text{dB}) = 10\log_{10}(P_s/\sigma^2)$. To simulate the PLC channel, we generate the impulsive noise with different IONs for different slots. To facilitate comparison, we consider three scenarios related to different average IONs, which are $A = 0.01, A = 0.1$, and $A = 0.5$. The number of PLC sub-channels L in Fig. 2 is 10. In addition, we set Γ as 0.01, 0.1, 0.5, and 10 by adjusting the pulse widths. The parameter of PLC channel fading a_0, a_1, and a_2 are set as 8.21, 12.37, and 0.02. The power of impulsive noise and Gaussian noise are set as -15 dB and 2.5 dB, respectively.

TABLE 1. Values of approximate parameters in (29).

L	a_0	a_1	a_2
2	23.91	24.67	0.00430
4	12.69	14.51	0.00995
6	10.13	12.81	0.0140
8	8.94	12.38	0.0172
10	8.21	12.37	0.02

To set up the simulation environment, we consider a PLC channel with three noise states. Specifically, ION equals 2, 6, and 10, respectively. Afterwards, we mix these three impulsive noises randomly to construct three testing environments including light, medium, and heavy impulsive noise environments. In the light impulsive noise environment, the proportions of the three impulsive noises, of which ION equals 2, 6, and 10, are respectively set as 94%, 5%, and 1%. In the medium impulsive noise environment, the proportions are set as 30%, 50%, and 20%. In the heavy impulsive noise environment, the proportions are set as 1%, 5%, and 94%, respectively. Finally, A in the three environments is around 0.5, 0.1, and 0.01, respectively. As a benchmark, we also consider the memoryless PLC channel, where the impulsive noise occurrence follows the Poisson distribution [27]. To compare the proposed PLC channel with memory with the memoryless PLC channel, the parameters for the memoryless PLC channel, such as ION, A, and L are set to be the same with those for the PLC channel with memory in the light impulsive noise environment.

According to Fig. 4, we construct a three-state Markov system given the three testing environments and the transition probability matrix is calculated according to (6). Furthermore, we derive $\boldsymbol{\varsigma}$ and $\boldsymbol{\rho}$ for the three testing environments, respectively. The inputs of the PLC channel with memory are Gaussian signals. Then, we obtain the achievable rates of the PLC channels with memory under the three testing environments using (17), as demonstrated in Fig. 5. The highest achievable rate of the memory PLC channel is achieved in the light impulsive noise environment. We observe that the achievable rate of the memoryless PLC channel is higher then that of the PLC channel with memory in the light impulsive noise environment. The reason is that the entropy between the input and output signals of the memoryless PLC channel is larger than that in the PLC channel with memory according to [27].

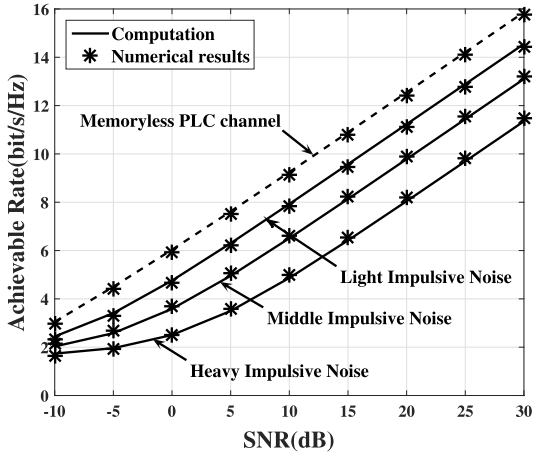

FIGURE 5. Achievable rate against transmit SNR of the PLC Channels with memory when IONs are different and $L = 10$.

To verify the ergodic capacity, we set the values of the parameters ω_i and q_i as shown in Table 2. Additionally, the accuracy of the results computed by (29) depends on J. A larger J can help to obtain a more accurate approximation while leading to a significant increase in complexity. In the following, we let $J = 10$.

Fig. 6 shows the ergodic capacity versus the transmit SNR for the PLC channel with memory in three testing environments. The analytical results are obtained by (29), which are consistent with those of Monte-Carlo. The decrease of A leads to a larger gap of the curves of the ergodic capacities. The reason is that the increase of the occurrence probability for the light impulsive noise state leads to the longer time for the system staying in the light impulsive noise state. For the same

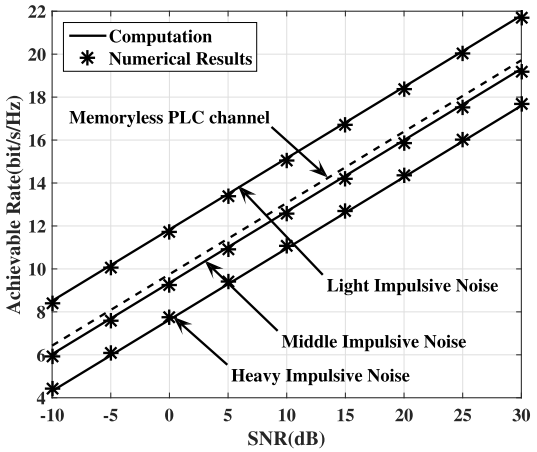

FIGURE 6. Ergodic capacity of the PLC channels with memory in three testing environments.

reason, the ergodic capacity of the PLC channel with memory is larger than that of the memoryless PLC channel, which is demonstrated in Fig. 6.

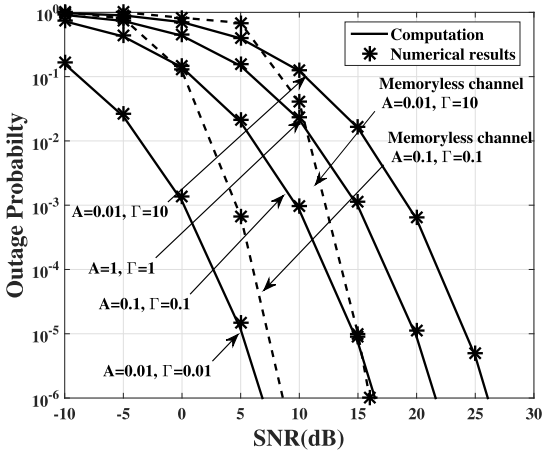

FIGURE 7. Outage probability of the PLC channel with memory with different parameters.

Fig. 7 shows the outage probability versus the transmit SNR for the PLC channels, which is obtained by (31). Similarly, the analytical and simulation results are consistent. The outage probability becomes worse with the increase of A or Γ. However, the outage probability of the PLC system is much better when Γ is reduced since the increase of Γ can reduce the received SNR dramatically. Meanwhile, the outage probability for the memoryless PLC channel is much better than that of the PLC channel with memory since the received SNR of the memoryless PLC channel is larger than that of the PLC channel with memory, even with the same A and Γ. Especially, the outage probability increases rapidly when Γ becomes very large, i.e., $\Gamma = 10$. This is because a large Γ indicates that the impulse is of a very long time duration, which results in a significant decrease of the received SNR.

VI. CONCLUSIONS

In this paper, we analyze the performance of PLC systems under impulsive noise. We model the PLC channel with memory as a Markov process and have derived its achievable rate by computing the conditional state probability and the achievable rate of each state. By adopting an accurate approximation for the lognormal sum functions, we obtain the CDF for the received SNR. Based on the CDF, we have developed expressions of the ergodic capacity and outage probability for the PLC channel with memory. Furthermore, we have verified the accuracy and the correctness of our analyses with numerical results.

APPENDIX A
PROOF OF THEOREM 1

Proof: First, we define the input and output sequences of the PLC channel as X^N and Y^N. Therefore, X^N can be given as $\{x_1, x_2, \cdots, x_N\}$, where x_n, $1 \le n \le N$ has N possibilities. For any X^N and Y^N, we can express their mutual information as $I\left(X^N; Y^N\right)$, which represents the amount of information. Therefore, if we can choose an X^N from all available input sequences, which ensures that the mutual information achieves its maximum value, the maximum mutual information is considered as the achievable rate of the PLC channel, expressed as

$$C = \lim_{N\to\infty} \max_{\Theta(X^N)} \frac{1}{N} I\left(X^N; Y^N\right), \tag{32}$$

where $\Theta\left(X^N\right)$ is the set of all available input sequences of X^N and $I\left(X^N; Y^N\right)$ represents the mutual information, given by

$$I\left(X^N; Y^N\right) = H\left(Y^N\right) - H\left(Y^N|X^N\right), \tag{33}$$

where the output entropy $H(Y) = E\left(-\log p\left(y\right)\right)$ and the conditional entropy $H\left(Y|X\right) = E\left(-\log p\left(y|x\right)\right)$.

Accordingly, we have

$$H\left(Y^N\right) = \sum_{n=1}^{N} H\left(Y_n|Y^{n-1}\right) \tag{34}$$

and

$$H\left(Y^N|X^N\right) = \sum_{n=1}^{N} H\left(Y_n|X_n, Y^{n-1}, X^{n-1}\right). \tag{35}$$

Substituting (34) and (35) into (32), we obtain

$$C = \lim_{N\to\infty} \max_{\Theta(X^N)} \frac{1}{N} \left(\sum_{n=1}^{N} H\left(Y_n|Y^{n-1}\right) - \sum_{n=1}^{N} H\left(Y_n|X_n, Y^{n-1}, X^{n-1}\right)\right). \tag{36}$$

With the definition of the conditional entropy, we have

$$H\left(Y_n|X_n, X^{n-1}, Y^{n-1}\right) = \mathbb{E}\left(-\log p\left(y_n|x_n, x^{n-1}, \ y^{n-1}\right)\right). \tag{37}$$

According to (8), we have

$$\log p\left(y_n|x_n, x^{n-1}, y^{n-1}\right) = \log \sum_{m=0}^{M-1} p\left(y_n|x_n, x^{n-1}, y^{n-1}, \ U_n = s_m\right). \quad (38)$$

With (35) and the property for the entropy of the continuous variable, we obtain

$$\mathbb{E}\left(-\log \sum_{m=0}^{M-1} p\left(y_n|x_n, x^{n-1}, y^{n-1}, U_n = s_m\right)\right) = -\int_0^{\infty} \log \sum_{m=0}^{M-1} p\left(y_n|x_n, U_n = s_m\right) p(U_n = s_m) d(y_n|x_n). \quad (39)$$

Since $p(y_n|x_n, U_n = s_m)$ depends on the noise of the mth state and the noise is Gaussian, we have

$$H\left(Y_n|X_n, X^{n-1}, Y^{n-1}\right) = \int_0^{\infty} \log \sum_{m=0}^{M-1} \varsigma_n(m) p\left(y_n|x_n, \ U_n = s_m\right) dx. \quad (40)$$

Since the sum of normal distributed variables is also normal distributed, the following expression holds

$$\int_0^{\infty} \log \sum_{m=0}^{M-1} \varsigma_i(m) p\left(y_n|x_n, U_n = s_m\right) dx = \log \sum_{m=0}^{M-1} \left(\pi e \sigma_m^2 \varsigma_n^2(m)\right). \quad (41)$$

With (11), (12), and (34), $H(Y_n|Y^{n-1})$ can be expressed as

$$H\left(Y_n|Y^{n-1}\right) = \int_0^{\infty} -\log \sum_{m=0}^{M-1} p\left(y_n|U_n = s_m\right) \times p\left(U_n = s_m|y^{n-1}\right) dy_n. \quad (42)$$

For the mth state, the noise is Gaussian and we assume that the source is Gaussian. Therefore, the received signal follows a Gaussian process and we have

$$\mathbb{E}\left(\log p\left(y_n|U_n = s_m\right)\right) = \int_0^{\infty} \log \frac{1}{\sqrt{2\pi P_r(m)}} e^{-\frac{x^2}{2P_r(m)}} dx = \log \pi e \sum_{m=0}^{M-1} \left((1+\gamma_m)\sigma_m^2 \rho_n^2(m)\right), \quad (43)$$

where P_r is the power of the received signal.

With the combination of (42) and (43), it follows that

$$H\left(Y_n|Y^{n-1}\right) = \log \sum_{m=0}^{M-1} \left(\pi e \sigma_m^2 \left(1+\gamma_m\right) \rho_n^2(m)\right). \quad (44)$$

Substituting (41) and (44) into (36), we obtain

$$R_{mry} = \frac{1}{N} \sum_{n=1}^{N} \left(\log \sum_{m=0}^{M-1} \left(\pi e \sigma_m^2 \left(1+\gamma_m\right) \rho_n^2(m)\right) - \log \sum_{m=0}^{M-1} \left(\pi e \sigma_m^2 \varsigma_n^2(m)\right)\right). \quad (45)$$

Hence, (17) holds, which completes the proof of Theorem 3. ■

APPENDIX B
PROOF OF THEOREM 2

Proof: In the following, we consider the ergodic capacity of PLC channels where the channel gains are given in (27). According to (17), the ergodic capacity of the PLC channel with memory can be written as

$$C_{mry} = \int_0^{\infty} C_D(x)\, dF_t(x) = \int_0^{\infty} \frac{1}{N} \sum_{n=1}^{N} \left(\log \sum_{m=0}^{M-1} \left(\frac{\left(1+\gamma_m\right) \rho_n^2(m)}{\varsigma_n^2(m)}\right)\right) d\Phi\left(a_0 - a_1 x^{-a_2/\lambda}\right). \quad (46)$$

In high SNR systems, $\frac{\sum_{l=1}^{L} h_l^2}{\sigma_m}$ is much larger than one and the integration is on $\left(a_0 - a_1(x)^{-a_2/\lambda}\right)$. Thus (46) can be transformed as

$$C_{mry} = \frac{1}{N} \sum_{n=1}^{N} \left(\log \left(\sum_{m=0}^{M-1} \frac{\rho_n^2(m)}{\sigma_m^2 \varsigma_n^2(m)}\right)\right) + \int_0^{\infty} \log x d\Phi\left(a_0 - a_1 x^{-a_2/\lambda}\right). \quad (47)$$

Define $s = a_0 - a_1 x^{-a_2/\lambda}$. (47) can be expressed as

$$C_{mry} = \frac{1}{N} \sum_{n=1}^{N} \left(\log \left(\sum_{m=0}^{M-1} \frac{\rho_n^2(m)}{\sigma_m^2 \varsigma_n^2(m)}\right) + \frac{1}{\sqrt{2\pi}} \int_{-\infty}^{\infty} \log \left(\left(\frac{a_0 - s}{a_1}\right)^{-\lambda/a_2}\right) e^{-\frac{s^2}{2}} ds\right). \quad (48)$$

According to (48), we obtain (29), which completes the proof of Theorem 5. ■

REFERENCES

[1] M. Sheikh-Hosseini, G. Abed Hodtani, and M. Molavi-Kakhki, "Capacity analysis of power line communication point-to-point and relay channels," *Trans. Emerg. Telecommun. Technol.*, vol. 27, no. 2, pp. 200–215, Jul. 2016.

[2] J. Anatory, N. Theethayi, R. Thottappillil, M. M. Kissaka, and N. H. Mvungi, "Broadband power-line communications: The channel capacity analysis," *IEEE Trans. Power Del.*, vol. 23, no. 1, pp. 164–170, Jan. 2008.

[3] Y. Qian, J. Li, Y. Zhang, and D. N. K. Jayakody, "Performance analysis of an opportunistic relaying power line communication systems," *IEEE Syst. J.*, to be published.

[4] Y. H. Ma, P. L. So, and E. Gunawan, "Performance analysis of OFDM systems for broadband power line communications under impulsive noise and multipath effects," *IEEE Trans. Power Del.*, vol. 20, no. 2, pp. 674–682, Apr. 2005.
[5] M. Zimmermann and K. Dostert, "A multipath model for the powerline channel," *IEEE Trans. Commun.*, vol. 50, no. 4, pp. 553–559, Apr. 2002.
[6] S. Guzelgoz, H. B. Celebi, and H. Arslan, "Statistical characterization of the paths in multipath PLC channels," *IEEE Trans. Power Del.*, vol. 26, no. 1, pp. 181–187, Jan. 2011.
[7] S. Galli, A. Scaglione, and Z. Wang, "For the grid and through the grid: The role of power line communications in the smart grid," *Proc. IEEE*, vol. 99, no. 6, pp. 998–1027, Jun. 2011.
[8] M. Antoniali, A. M. Tonello, M. Lenardon, and A. Qualizza, "Measurements and analysis of PLC channels in a cruise ship," in *Proc. IEEE Int. Symp. Power Line Commun. Appl. (ISPLC)*, Udine, Italy, Apr. 2011, pp. 102–107.
[9] H. C. Ferreira, L. Lampe, J. Newbury, and T. G. Swart, *Power Line Communications: Theory and Applications for Narrowband and Broadband Communications Over Power Lines*. Singapore: Wiley, 2010.
[10] L. Lampe and A. J. H. Vinck, "On cooperative coding for narrow band PLC networks," *AEU-Int. J. Electron. Commun.*, vol. 65, no. 8, pp. 681–687, Apr. 2011.
[11] X. Cheng, R. Cao, and L. Yang, "Relay-aided amplify-and-forward powerline communications," *IEEE Trans. Smart Grid*, vol. 4, no. 1, pp. 265–272, Mar. 2013.
[12] A. Dubey, R. K. Mallik, and R. Schober, "Performance analysis of a power line communication system employing selection combining in correlated log-normal channels and impulsive noise," *IET Commun.*, vol. 8, no. 7, pp. 1072–1082, May 2014.
[13] M. Ghosh, "Analysis of the effect of impulse noise on multicarrier and single carrier QAM systems," *IEEE Trans. Commun.*, vol. 44, no. 2, pp. 145–147, Feb. 1996.
[14] J. Haring and A. Vinck, "OFDM transmission corrupted by impulsive noise," in *Proc. IEEE Int. Symp. PLC Appl.*, Apr. 2000, pp. 9–14.
[15] R. Pighi, M. Franceschini, G. Ferrari, and R. Raheli, "Fundamental performance limits of communications systems impaired by impulse noise," *IEEE Trans. Commun.*, vol. 57, no. 1, pp. 171–182, Jan. 2009.
[16] A. Chopra, K. Gulati, B. L. Evans, K. R. Tinsley, and C. Sreerama, "Performance bounds of MIMO receivers in the presence of radio frequency interference," in *Proc. IEEE ICASSP*, Taipei, Taiwan, Apr. 2009, pp. 2817–2820.
[17] S. P. Herath, N. H. Tran, and T. Le-Ngoc, "On optimal input distribution and capacity limit of Bernoulli–Gaussian impulsive noise channels," in *Proc. IEEE ICI*, Ottawa, ON, Canada, Nov. 2012, pp. 3429–3433.
[18] S. P. Herath, N. H. Tran, and T. Le-Ngoc, "Optimal signaling scheme and capacity limit of PLC under Bernoulli–Gaussian impulsive noise," *IEEE Trans. Power Del.*, vol. 30, no. 1, pp. 97–105, Aug. 2015.
[19] K. C. Wiklundh, P. F. Stenumgaard, and H. M. Tullberg, "Channel capacity of Middleton's class A interference channel," *Electron. Lett.*, vol. 45, no. 24, pp. 1227–1229, Nov. 2009.
[20] B. Nikfar, T. Akbudak, and A. J. H. Vinck, "MIMO capacity of class a impulsive noise channel for different levels of information availability at transmitter," in *Proc. 18th IEEE Int. Symp. Power Line Commun. Appl.*, Mar. 2014, pp. 266–271.
[21] A. J. Goldsmith and P. P. Varaiya, "Capacity, mutual information, and coding for finite-state Markov channels," *IEEE Trans. Inf. Theory*, vol. 42, no. 3, pp. 868–886, May 1996.
[22] D. G. Brennan, "Linear diversity combining techniques," *Proc. IEEE*, vol. 91, no. 2, pp. 331–356, Feb. 2003.
[23] F. J. C. Corripio, J. A. C. Arrabal, L. D. del Rio, and J. T. E. Munoz, "Analysis of the cyclic short-term variation of indoor power line channels," *IEEE J. Sel. Areas Commun.*, vol. 24, no. 7, pp. 1327–1338, Jul. 2006.
[24] G. Bumiller, L. Lampe, and H. Hrasnica, "Power line communication networks for large-scale control and automation systems," *IEEE Commun. Mag*, vol. 48, no. 4, pp. 106–113, Apr. 2010.
[25] N. C. Beaulieu and F. Rajwan, "Highly accurate simple closed-form approximations to lognormal sum distributions and densities," *IEEE Commun. Lett.*, vol. 8, no. 12, pp. 709–711, Dec. 2004.
[26] "Homeplug AV white paper," HomePlug Powerline Alliance Inc., Tech. Rep., 2005.
[27] Y. Qian, H. Xie, X. Zhou, and F. Zhang, "Achievable rate and ergodic capacity for power line communication systems under impulsive noise," in *Proc. IEEE ICC Workshops*, Kansas City, MO, USA, May 2018, pp. 1–6.

YUWEN QIAN received the Ph.D. degree in automatic engineering from the Nanjing University of Science and Technology, Nanjing, China, in 2011. From 2002 to 2011, he was a Lecturer with the Automation School, Nanjing University of Science and Technology, where he has been a Lecturer with the School of Electronic and Optical Engineering since 2011. His main research interests are information security, smart grid, and power line communications.

XIANGWEI ZHOU received the B.S. degree in communication engineering from the Nanjing University of Science and Technology, Nanjing, China, in 2005, the M.S. degree in information and communication engineering from Zhejiang University, Hangzhou, China, in 2007, and the Ph.D. degree in electrical and computer engineering from the Georgia Institute of Technology, Atlanta, GA, USA, in 2011. He was an Assistant Professor with the Department of Electrical and Computer Engineering, Southern Illinois University, Carbondale, IL, USA, from 2013 to 2015, and a Senior Systems Engineer with Marvell Semiconductor, Santa Clara, CA, USA, from 2011 to 2013. Since 2015, he has been an Assistant Professor with the Division of Electrical and Computer Engineering, Louisiana State University, Baton Rouge, LA, USA. His research interests include wireless communications, statistical signal processing, and cross-layer optimization, with current emphasis on spectrum-efficient, energy-efficient and secure communications, coexistence of wireless systems, and machine learning for intelligent communications. He was a recipient of the Best Paper Award at the 2014 International Conference on Wireless Communications and Signal Processing.

JUN LI received the Ph.D. degree in electronic engineering from Shanghai Jiao Tong University, Shanghai, China, in 2009. In 2009, he was with the Department of Research and Innovation, Alcatel Lucent Shanghai Bell, as a Research Scientist. From 2009 to 2012, he was a Post-Doctoral Fellow with the School of Electrical Engineering and Telecommunications, University of New South Wales, Australia. From 2012 to 2015, he was a Research Fellow with the School of Electrical Engineering, The University of Sydney, Australia. Since 2015, he has been a Professor with the School of Electronic and Optical Engineering, Nanjing University of Science and Technology, Nanjing, China. His research interests include network information theory, channel coding theory, wireless network coding, and resource allocations in cellular networks.

FEIXIANG ZHANG received the B.S. and M.S. degrees in optics from the Harbin Institute of Technology, Harbin, China, in 2010 and 2012, respectively. He is currently pursuing the Ph.D. degree with the Division of Electrical and Computer Engineering, Louisiana State University. He received the Best Paper Award from the International Conference on Wireless Communications and Signal Processing in 2014. He was a recipient of the 2015 James R. Lewis Fellowship awarded by the Division of Electrical and Computer Engineering, Louisiana State University.

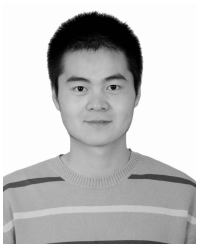

LONG SHI (S'10–M'13) received the Ph.D. degree in electrical engineering from the University of New South Wales, Sydney, Australia, in 2012. He was a Visiting Student with The Chinese University of Hong Kong in 2010 and the University of Delaware in 2011. From 2013 to 2016, he was a Post-Doctoral Fellow with the Institute of Network Coding, The Chinese University of Hong Kong. From 2014 to 2017, he was a Lecturer with the College of Electronic and Information Engineering, Nanjing University of Aeronautics and Astronautics. He is currently a Post-Doctoral Research Fellow with the Singapore University of Technology and Design. His current research interests include wireless caching, wireless network coding, and channel coding.

FENG SHU received the B.S. degree from Fuyang teaching College, Fuyang, China, in 1994, the M.S. degree from Xidian University, Xian, China, in 1997, and the Ph.D. degree from Southeast University, Nanjing, in 2002. From 2003 to 2005, he was a Post-Doctoral Researcher with the National Key Mobile Communication Laboratory, Southeast University. In 2005, he joined the School of Electronic and Optical Engineering, Nanjing University of Science and Technology, Nanjing, China, where he is currently a Professor and a Supervisor of Ph.D. and graduate students. From 2009 to 2010, he held a visiting post-doctoral position with The University of Texas at Dallas. His research interests include wireless networks, wireless location, and array signal processing.